RESEARCH ARTICLE

A comparative study on the estimation of ultimate bearing capacity of rock masses using finite element and limit equilibrium methods

Serdar Koltuk*

Technical University of Berlin, Ernst-Reuter-Platz 1, Berlin and 10587, Germany, ORCID:0000-0002-6214-0848

Abstract

Most rock masses are excellent foundation materials due to their bearing capacities of MPa. However, the ultimate bearing capacity of rock masses should be accurately estimated in the design of structures with high foundation loads. In this study, the ultimate bearing capacities of a strip footing built on rock masses with different geotechnical properties are determined using the finite element method (FEM) and the failure criterion of Hoek & Brown. The results of FE-analyses are compared to those obtained from the limit equilibrium methods (LEM) in the literature. It has been shown that the FEM with associated flow rule and Terzaghi`s limit equilibrium method give similar failure surfaces for most cases, and the ratio of ultimate bearing capacities determined according to the Terzaghi´s method to FEM varies between 1.5 and 4. In cases, in which the failure surfaces obtained from both methods differ, this ratio can rise up to 11.

1. Introduction

Most rock masses are excellent foundation materials due to their bearing capacities of MPa. However, in the design of structures with high foundation loads such as high-rise buildings, dams and viaduct piers, the ultimate bearing capacities of rock masses should be accurately estimated.

———————

* Corresponding author. Tel.: +491634677933
  E-mail address: serdar.koltuk@campus.tu-berlin.de
  https://www.tu.berlin/ingenieurgeologie/ueber-uns

.

Because of discontinuities existing in rock masses, the estimation of their bearing capacities is more difficult than soils. Various methods can be found in the literature to estimate the ultimate bearing capacity of shallow footings built on rock masses. These can be grouped under 4 main groups: Limit equilibrium, Slip-line, Limit analysis and Numerical methods [1-6]. In addition, the bearing capacities of certain rock types can be estimated empirically with the help of diagrams developed depending on the unconfined compressive strengths of intact rocks and the widths of openings existing in rock masses [7].

Terzaghi`s limit equilibrium method [1] with the failure criterion of Mohr-Coulomb is widely used by engineers working in construction practice to estimate the ultimate bearing capacity of shallow foundations. Bowles [8] pointed out that intact rock samples are used in the laboratory to determine the shear strength parameters (c and ϕ) so that they do not account for the effect of discontinuities existing in rock masses. Therefore, he suggested that ultimate bearing capacities calculated according to the Terzaghi`s approach should be reduced.

It is known that the shear strengths of most rocks are significantly affected by stress levels. Furthermore, rocks have significant tensile strengths compared to soils. Among the nonlinear failure criteria in the literature, the criterion of Hoek and Brown reliably simulates the deformation behavior of isotropic rocks [9,10]. Miranda et al. [11] combined the limit equilibrium method suggested by Wyllie [2] with the Hoek & Brown failure criterion.

The numerical methods have become widely used for solving complex engineering problems. In the last two decades, a growing use of numerical methods with the Hoek & Brown criterion have been observed to estimate the bearing capacities of rock masses.

In the recent studies, Javid, Fahimifar and Imani [12] investigated the effect of the interaction between two shallow strip footings on the ultimate bearing capacity using the Hoek & Brown criterion and two-dimensional numerical analyses. It has been seen that the ratio of the bearing capacity of a strip footing under the effect of a neighboring footing to the bearing capacity of the same isolated footing is about 1.3 to 1.6. Mansouri, Imani and Fahimifar [13] studied the ultimate bearing capacity of square- and rectangular-shaped footings with the help of the Hoek and Brown criterion and three-dimensional numerical analyses. It has been shown that the ultimate bearing capacities obtained from the 2D-analyses are higher than in the 3D-analyses. Shamloo and Imani [14] demonstrated that the effect of embedment depths on the bearing capacity of footings in rock masses cannot be taken into account correctly with the aid of equivalent surface loads. Using a self-developed adaptive finite element limit analysis code, Wu et al. [15] studied the ultimate bearing capacity of footings subjected to eccentric loads in rock masses with voids. To estimate the bearing capacity of strip footings on rock masses under three-dimensional effect, Chen, Zhu and Zhang [16] developed an analytical method using the failure criterion of Hoek & Brown. Ranjbarnia, Zarei and Goudarzy [17] introduced a probabilistic approach to estimate the bearing capacity of shallow foundations on rock masses. Das and Chakraborty [18] developed the design charts to estimate the bearing capacity of strip foundations with eccentric and inclined loads. Chen, Zhu and Zhang [19] demonstrated that ignoring the three-dimensional strength and the weight of rock mass would lead to the underestimation of the bearing capacity of rock masses.

In the present study, the ultimate bearing capacity of a strip footing on rock masses with different geotechnical properties was estimated using the finite element method (FEM) with the failure criterion of Hoek & Brown. The results of the FE-analyses are compared to those obtained from the limit equilibrium methods (LEM) suggested by Terzaghi [1] and Miranda et al. [11]. The present study shows engineers working in construction practice the limits of the use of limit equilibrium methods in determining the bearing capacity of rock masses.

2. Methodology

2.1. Numerical method

The software Plaxis-2D [20], which is based on the finite element method, is used to estimate the ultimate bearing capacity of a strip footing on rock masses.

Numerical model:

By utilizing the symmetry feature, only half of the numerical model shown in Figure 1 was created. Pre-analyses have shown that the size effect of the model on the numerical results can be ignored if the horizontal and vertical lengths of the model were not smaller than 12.5 m and 10 m, respectively. The lateral boundaries were fixed in the horizontal direction while the bottom boundary was fixed in the both directions. A rigid strip footing was modeled as a continuous load with a width of 0.5 m on the rock surface without an embedment depth. In order to model a rough footing, the horizontal movement of the footing was prevented. In the vertical direction, a deformation value leading to the ground failure was inputted. The ground water level was defined at the base of the model, and the moist unit weight of the rock masses was set to 24 kN/m^3.
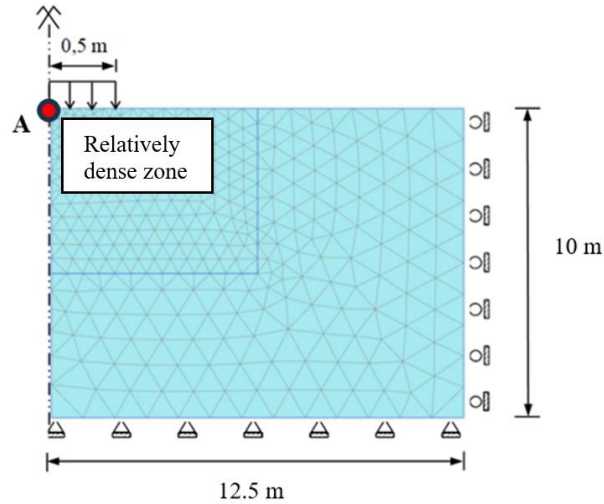
Fig. 1. FE-model in Plaxis 2D.

The effect of mesh density on the numerical results is well known. A dense mesh causes prolonged analysis time and an uneconomical solution while the use of a relatively loose mesh affects the accuracy of numerical results. In Plaxis-2D [20], the generation of FE-mesh is fully automated and a robust triangulation procedure. Pre-analyses have shown that a relatively dense mesh generated in the area of 5 m x 6 m under the foundation load in Fig. 1 allowed the numerical results to converge to a constant value. As a result, 942 triangular elements with 15 nodes and an average element size of 0.42 m were generated in the numerical model.

The analyses consisted of 2 stages. In the first step, the initial stress condition existing in the rock mass before the foundation load was reconstructed using the K0-procedure. The second stage was the plastic calculation stage, in which the reaction force of the rock mass corresponding to the deformation inputted in the vertical direction was determined. To determine the ultimate bearing capacity, the graph of the reaction force-deformation obtained for Point A was considered. In this graph, twice the maximum load that converges to a constant value, which was determined using the method of tangent intersection defined by Singh et al. [21], was assumed to be q_{ult}.

Constitutive model:

In Plaxis-2D [20], the stress-strain behaviors of rock masses were modeled using the criterion of Hoek and Brown. The empirical equation proposed by Hoek for intact rocks is expressed as follows [9,10]:

$$\sigma_1 = \sigma_3 + \sigma_{ci} \cdot (m_i \cdot \frac{\sigma_3}{\sigma_{ci}} + 1)^{0,5} \tag{1}$$

where σ_{ci} is the unconfined compressive strength of intact rock, m_i is material constant for intact rock, which is determined experimentally. Depending on the rock type, it can take values between 2 and 35.

Later, the Hoek`s criterion was developed by Brown for jointed rock masses, and it is called the Hoek-Brown failure criterion. Hoek-Brown [9,10] generalized failure criterion is expressed by Eq. (2):

$$\sigma_1 = \sigma_3 + \sigma_{ci} \cdot \left(m_b \cdot \frac{\sigma_3}{\sigma_{ci}} + s\right)^a \tag{2}$$

where the parameters "m_b, s and a" are the material constants for rock mass and can be calculated by using Eq. (3)-(5):

$$s = e^{\left(\frac{GSI-100}{9-3D}\right)} \tag{3}$$

$$a = 0,5 + 0,167 \cdot \left(e^{\frac{-GSI}{15}} - 0,0013\right) \tag{4}$$

$$m_b = m_i \cdot e^{\left(\frac{GSI-100}{28-14D}\right)} \tag{5}$$

where GSI is Geological Strength Index, D is disturbance factor.

The geological strength index of the rock mass is determined visually depending on the structure of rock masses and their surface properties. The GSI-values vary between 0 for rocks that have decomposed into the soil and 100 for intact rocks with unweathered surfaces. A chart for determining GSI -value is given by Hoek and Brown [10]. The value of the disturbance factor varies between 0 (for undisturbed rocks) and 1 (for disturbed rocks by excavations or explosion etc.).

The Hoek & Brown failure criterion should be used for intact rocks, rock masses with several discontinuities and heavily jointed rock masses (Group I and III) which have similar surface properties and can be considered isotropic [5]. Furthermore, this failure criterion was based on the brittle failures observed in triaxial tests on intact rocks. Therefore, it should not be used for principal stress levels at which ductile failure appears [9,10]. Furthermore, it should not be used if the size of the rock blocks is larger than the structure or they have same size or if one group of discontinuities existing in the rock mass is weaker than the others [5,12].

Eight parameters must be inputted in Plaxis-2D [20]. These parameters are: 1) Young's modulus of rock mass E_{rm}, 2) Poisson's ratio of rock mass ν, 3) unconfined compressive strength of intact rock σ_{ci}, 4) material constant for intact rock m_i, 5) geological strength index of rock mass GSI, 6) disturbance factor D, 7) dilation angle of rock mass φ_{max} for zero confining pressure, and 8) confining pressure σ_φ at the depth, where the dilation angle is equal to zero.

The Young's modulus E_{rm} can be calculated based on the GSI and D values with the help of the following simplified equation:

$$E_{rm}(MPa) = 10^5 \cdot \left(\frac{1-\frac{D}{2}}{1+e^{\left(\frac{75+25D-GSI}{11}\right)}}\right) \tag{6}$$

Poisson's ratio ν varies between 0.1 and 0.4 depending on the rock type. In this study, the value of ν was taken as 0.2. Since the foundation used in the numerical model has no embedment depth, there will be no excavation, and thus no disturbance occurs in the rock mass. Therefore, the value of D was taken as 0. In the analyses, the unconfined compressive strength σ_{ci} of intact rock was considered with 4 different values σ_{ci} = 1, 5, 25, 100 MPa, the material constant m_i of intact rock with 3 different values m_i = 2.5, 10, 20, and the geological strength index of rock mass GSI with 5 different values GSI = 10, 30, 50, 70, 90.

Rock masses show dilatation behaviour when they are subjected to shearing under low confining pressures. In this study, the value of φ_{max} was set to the friction angle of the rock mass, and its value was decreased linearly to 0 at a certain depth (associated flow) [20]. The confining stress at the depth where the dilation angle is zero was set to $\sigma_{\varphi} = 1000$ kN/m^2 taking into account that the vertical length of the model and the unit weight of rock masses were 10 m and 24 kN/m^3, respectively.

2.2. Limit equilibrium method

In the present study, the limit equilibrium methods suggested by Terzaghi [1] and Miranda et al. [11] are used to estimate the ultimate bearing capacities of rock masses.

Terzaghi`s method:
Terzaghi [1,22] proposed the failure surface under a strip foundation whose width B is very small compared to its length (see Figure 2a). This failure surface consists of 3 zones: 1) a triangular zone ACD, 2) radial shear zones AFD and CDE with logarithmic spirals DE and DF, 3) Rankine triangular passive zones AFH and CEG. The ultimate bearing capacity q_{ult} is obtained by considering the equilibrium of the triangular wedge ACD and using the failure criterion of Mohr-Coulomb as follow:

$$q_{ult} = c \cdot N_c + \gamma \cdot D_f \cdot N_q + 0.5 \cdot \gamma \cdot B \cdot N_\gamma \tag{7}$$

where c is cohesion, γ is unit weight of rock mass, D_f is foundation depth, B is foundation width, N_c, N_q and N_γ are bearing capacity factors that can be calculated by using Eqs. (8)-(10) depending on the friction angle ϕ of the rock mass:

$$N_c = 5 \cdot tan^4 \left(45 + \frac{\phi}{2} \right) \tag{8}$$

$$N_q = tan^6 \left(45 + \frac{\phi}{2} \right) \tag{9}$$

$$N_\gamma = N_q + 1 \tag{10}$$

Miranda`s method:
Miranda et al. [11] combined Wyllie`s limit equilibrium method [2] with the Hoek & Brown failure criterion. In Figure 2b, the wedge A is the active wedge and the wedge B is the passive wedge, which are representing the failure zones under a strip footing. In this method, the weights of the rock masses and the shear stresses that develop at the interface of both wedges are neglected. The wedges A and B are assumed to be in compression as in triaxial shear tests.
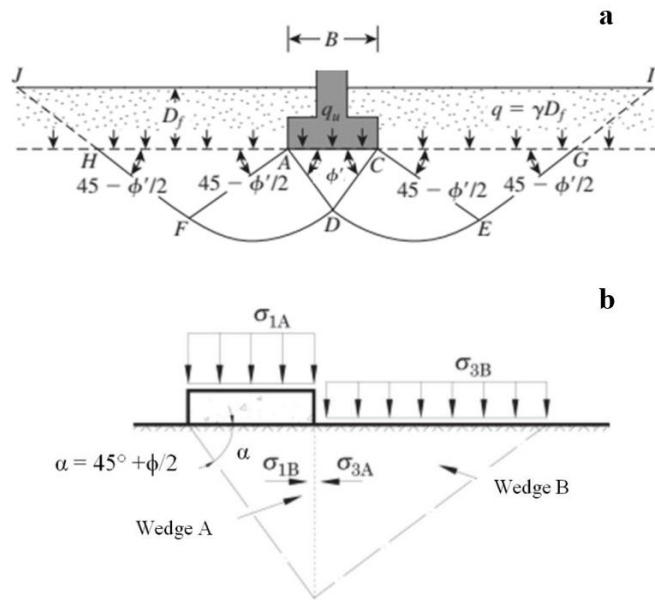
Fig. 2. Ultimate bearing capacity of rock masses according to (a) Terzaghi [22]; (b) Wyllie [2].

Assuming that there is no load on the rock surface outside the foundation area, the major and minor principal stresses in the wedge B will act in the horizontal direction (σ_{1B}) and in the vertical direction ($\sigma_{3B} = 0$), respectively. When the wedge A collapses, the minor principal stress σ_{3A} acting on the wedge A will be equal to the major principal stress σ_{1B} in the wedge B. Therefore, the major principal stress σ_{1A} in the wedge A will correspond to the ultimate bearing capacity q_{ult} of the footing.

In the Miranda`s method, by substituting $\sigma_3 = \sigma_{3B} = 0$ in Eq. (2), the following equation is firstly obtained for the wedge B:

$$\sigma_{1B} = \sigma_{ci} \cdot s^a$$
(11)

Then, substituting $\sigma_3 = \sigma_{3A} = \sigma_{ci} \cdot s^a$ in Eq. (2), the following equation is obtained for the wedge A, which gives the ultimate bearing capacity q_{ult}:

$$q_{ult} = \sigma_{1A} = \sigma_{ci} \cdot [s^a + (m_b \cdot s^a + s)^a]$$
(12)

3. Results and discussion

3.1. Comparison of the failure surfaces obtained from the FEM and LEM

The numerical analyses carried out in this study gave three different failure surfaces, as shown in Fig. 3. These failure surfaces were called failure type A, B, and C. A summary of the failure types observed in the FE-analyses with associated flow is given in Table 1 depending on the Hoek & Brown parameters.
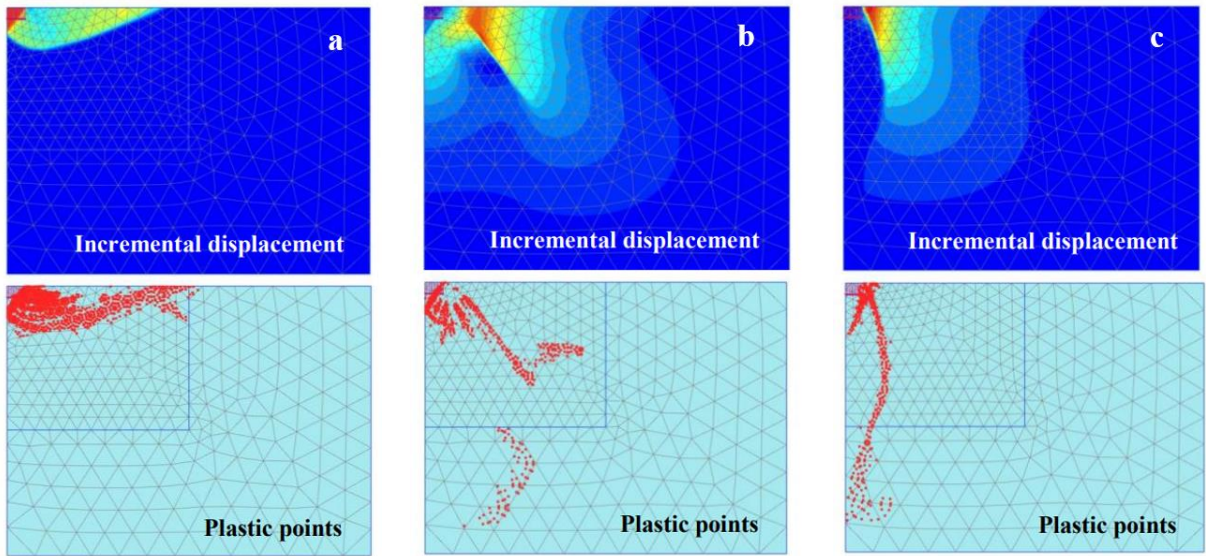
Fig. 3. Failure surfaces obtained from the FE-analyses: (a) failure type A, (b) failure type B, (c) failure type C.

A total of 60 analyses were performed, and the most of these analyses gave a failure zone shown in Fig. 3a (Failure type A). This failure zone corresponds to the general shear failure suggested by Terzaghi in Fig. 2a.

Only in 3 analyses (σ_{ci} = 25 MPa, m_i = 10, GSI = 30; σ_{ci} = 25 MPa, m_i = 10, GSI = 90 and σ_{ci} = 100 MPa, m_i = 20, GSI = 10), the Rankine triangular passive zone did not develop while the triangular zone and radial shear zone developed. The failure type B shown in Fig. 3b is a local shear failure.

In 12 analyses (σ_{ci}=100 MPa, m_i = 10, GSI = 10 – 90; σ_{ci} = 100 MPa, m_i = 20, GSI = 30 – 90; σ_{ci} = 25MPa, m_i = 20, GSI = 70 – 90 and σ_{ci} = 25 MPa, m_i = 10, GSI = 50), the failure surface shown in Figure 3c appeared. Compared to the failure type A, a triangular wedge under the foundation appeared more deeply while the other zones of the Terzagi`s failure surface did not develop (punching failure). On the other hand, a new failure surface developed in vertical direction towards the inner part of the rock mass.

When the failure surfaces obtained from the FEM are examined, it is seen that the failure mechanism proposed by Wyllie [2,11] in Fig. 2b does not develop. Therefore, only the q_{ult} - values calculated according to the Terzaghi`s approach were used for comparison in Figure 4.

Table 1. Failure types depending on the Hoek & Brown parameters.

Rock parameters		GSI (-)				
σ_{ci} (MPa)	m_i (-)	10	30	50	70	90
	2.5	**A**	**A**	**A**	**A**	**A**
1	10	**A**	**A**	**A**	**A**	**A**
	20	**A**	**A**	**A**	**A**	**A**
	2.5	**A**	**A**	**A**	**A**	**A**
5	10	**A**	**A**	**A**	**A**	**A**
	20	**A**	**A**	**A**	**A**	**A**
	2.5	**A**	**A**	**A**	**A**	**A**
25	10	**A**	**B**	**C**	**A**	**B**
	20	**A**	**A**	**A**	**C**	**C**
	2.5	**A**	**A**	**A**	**A**	**A**
100	10	**C**	**C**	**C**	**C**	**C**

20	**B**	**C**	**C**	**C**	**C**

3.2. Comparison of the ultimate bearing capacities obtained from the FEM and LEM

In order to make a comparison between the results of the FEM and the Terzaghi`s method, the equivalent parameters of the Mohr-Coulomb criterion (c and ϕ) corresponding to the Hoek-Brown parameters used in the FE-analyses should be determined. The parameters of Mohr-Coulomb are calculated by plotting a linear envelope on the nonlinear failure envelope of Hoek and Brown that provides the best fit for a given stress range.

Table 2. Equivalent Mohr-Coulomb parameters for $m_i = 2.5$.

GSI (-)	σ_{ci} (MPa)							
	1		5		25		100	
	c (MPa)	ϕ (°)	c (MPa)	ϕ (°)	c (MPa)	ϕ (°)	c (MPa)	ϕ (°)
10	0.01	9.5	0.05	9.5	0.25	9.5	1.00	9.5
30	0.02	15.0	0.11	15.0	0.52	15.0	2.09	15.0
50	0.03	19.5	0.17	19.5	0.83	19.5	3.34	19.5
70	0.06	24.0	0.31	24.0	1.54	24.0	6.16	24.0
90	0.17	26.5	0.83	26.5	4.14	26.5	16.57	26.5

Table 3. Equivalent Mohr-Coulomb parameters for $m_i = 10$.

GSI (-)	σ_{ci} (MPa)							
	1		5		25		100	
	c (MPa)	ϕ (°)	c (MPa)	ϕ (°)	c (MPa)	ϕ (°)	c (MPa)	ϕ (°)
10	0.02	18.0	0.10	18.0	0.48	18.0	1.92	18.0
30	0.04	24.5	0.18	24.5	0.88	24.5	3.52	24.5
50	0.05	30.5	0.25	30.5	1.25	30.5	4.98	30.5
70	0.07	36.5	0.36	36.5	1.78	36.5	7.11	36.5
90	0.13	41.5	0.64	41.5	3.21	41.5	12.83	41.5

Table 4. Equivalent Mohr-Coulomb parameters for $m_i = 20$.

GSI (-)	σ_{ci} (MPa)							
	1		5		25		100	
	c (MPa)	ϕ (°)	c (MPa)	ϕ (°)	c (MPa)	ϕ (°)	c (MPa)	ϕ (°)
10	0.03	23.5	0.13	23.5	0.65	23.5	2.59	23.5
30	0.05	30.5	0.23	30.5	1.12	30.5	4.49	30.5
50	0.06	36.5	0.31	36.5	1.54	36.5	6.14	36.5
70	0.08	42.5	0.41	42.5	2.05	42.5	8.22	42.5
90	0.13	48.0	0.63	48.0	3.16	48.0	12.65	48.0

In this study, the equivalent Mohr-Coulomb parameters were calculated using the Software RocData [23]. Here, the "General" option was selected as the failure envelope interval, and the equivalent Mohr-Coulomb parameters were determined for the stress range of $0 < \sigma_3 < 0.25 \cdot \sigma_{ci}$, in which a brittle failure appears. The equivalent parameters of Mohr-Coulomb (c and ϕ) corresponding to the parameters of Hoek-Brown are given in Tables 2-4.

In Tables 5-7, the ultimate bearing capacities obtained from the finite element method (FEM) and limit equilibrium methods (LEM) are given depending on the various rock mass properties. As it can be seen from Tables

5-7, Terzaghi`s approach [1] gives the highest values of ultimate bearing capacity while the lowest values are obtained from the Miranda`s method. Only in 3 analyses (σ_{ci} = 25 MPa, m_i = 20, GSI = 90; σ_{ci} = 100 MPa, m_i = 20, GSI = 90 and σ_{ci} = 100 MPa, m_i = 20, GSI = 70), the q_{ult}-values calculated according to Miranda`s method are negligibly larger than the values in the FEM.

Table 5. Ultimate bearing capacities obtained from the FEM and LEM for m_i = 2.5.

GSI (-)	σ_{ci} (MPa)											
	1			5			25			100		
	Ultimate Bearing Capacity q_{ult} (MPa)											
	FEM	Miranda et al.	Terzaghi	FEM	Miranda et al.	Terzaghi	FEM	Miranda et al.	Terzaghi	FEM	Miranda et al.	Terzaghi
10	0.07	0.01	0.14	0.24	0.05	0.54	0.85	0.25	2.51	2.70	1	9.78
30	0.25	0.07	0.37	0.93	0.35	1.58	3.95	1.75	7.58	14.65	7	29.94
50	0.53	0.23	0.78	2.35	1.15	3.50	10.80	5.75	17.01	42.38	23	64.51
70	1.20	0.63	1.93	5.70	3.15	8.85	27.75	15.75	43.51	110.75	63	173.22
90	2.95	1.73	5.87	14.40	8.65	28.21	71.45	43.25	139.94	286.00	173	559.39

Table 6. Ultimate bearing capacities obtained from the FEM and LEM for m_i = 10.

GSI (-)	σ_{ci} (MPa)											
	1			5			25			100		
	Ultimate Bearing Capacity q_{ult} (MPa)											
	FEM	Miranda et al.	Terzaghi	FEM	Miranda et al.	Terzaghi	FEM	Miranda et al.	Terzaghi	FEM	Miranda et al.	Terzaghi
10	0.28	0.02	0.43	0.84	0.10	1.81	2.85	0.50	8.74	3.30	2	34.54
30	0.75	0.13	1.21	2.65	0.65	5.38	8.63	3.25	26.13	25.02	13	103.87
50	1.40	0.38	2.72	5.74	1.90	12.10	20.20	9.50	58.85	73.47	38	234.11
70	2.80	1.01	6.21	12.21	5.05	27.92	54.85	25.25	136.24	140.38	101	542.61
90	6.05	2.66	16.73	28.60	13.30	77.88	120.11	66.50	384.26	373.10	266	1532.15

Table 7. Ultimate bearing capacities obtained from the FEM and LEM for m_i = 20.

GSI (-)	σ_{ci} (MPa)											
	1			5			25			100		
	Ultimate Bearing Capacity q_{ult} (MPa)											
	FEM	Miranda et al.	Terzaghi	FEM	Miranda et al.	Terzaghi	FEM	Miranda et al.	Terzaghi	FEM	Miranda et al.	Terzaghi
10	0.55	0.03	0.88	1.81	0.15	3.75	5.35	0.75	17.98	12.45	3	71.0
30	1.34	0.17	2.45	4.70	0.85	10.88	18.15	4.25	52.74	31.05	17	209.21
50	2.61	0.51	5.48	9.80	2.55	24.55	34.20	12.75	119.81	55.12	51	476.45
70	4.65	1.34	12.51	20.10	6.70	56.21	40.89	33.50	274.42	127.14	134*	1092.52
90	9.10	3.47	32.32	42.50	17.35	146.65	81.79	86.75*	718.54	386.06	347*	2863.07

In the most FE-analyses, the vertical deformations occurring in the rock masses under the loads corresponding to

the ultimate bearing capacity of the footing were smaller than 2 cm. Only in 12 analyses (σ_{ci} = 100 MPa, m_i = 2.5, GSI = 70-90; σ_{ci} = 100 MPa, m_i = 2.5-10, GSI = 50; σ_{ci} = 100 MPa, m_i = 2.5-20, GSI = 30; σ_{ci} = 100 MPa, m_i = 2.5-10, GSI = 10; σ_{ci} = 25 MPa, m_i = 10-20, GSI = 10 and σ_{ci} = 25 MPa, m_i = 20, GSI = 30), the vertical deformations varied between 2 cm – 9 cm.
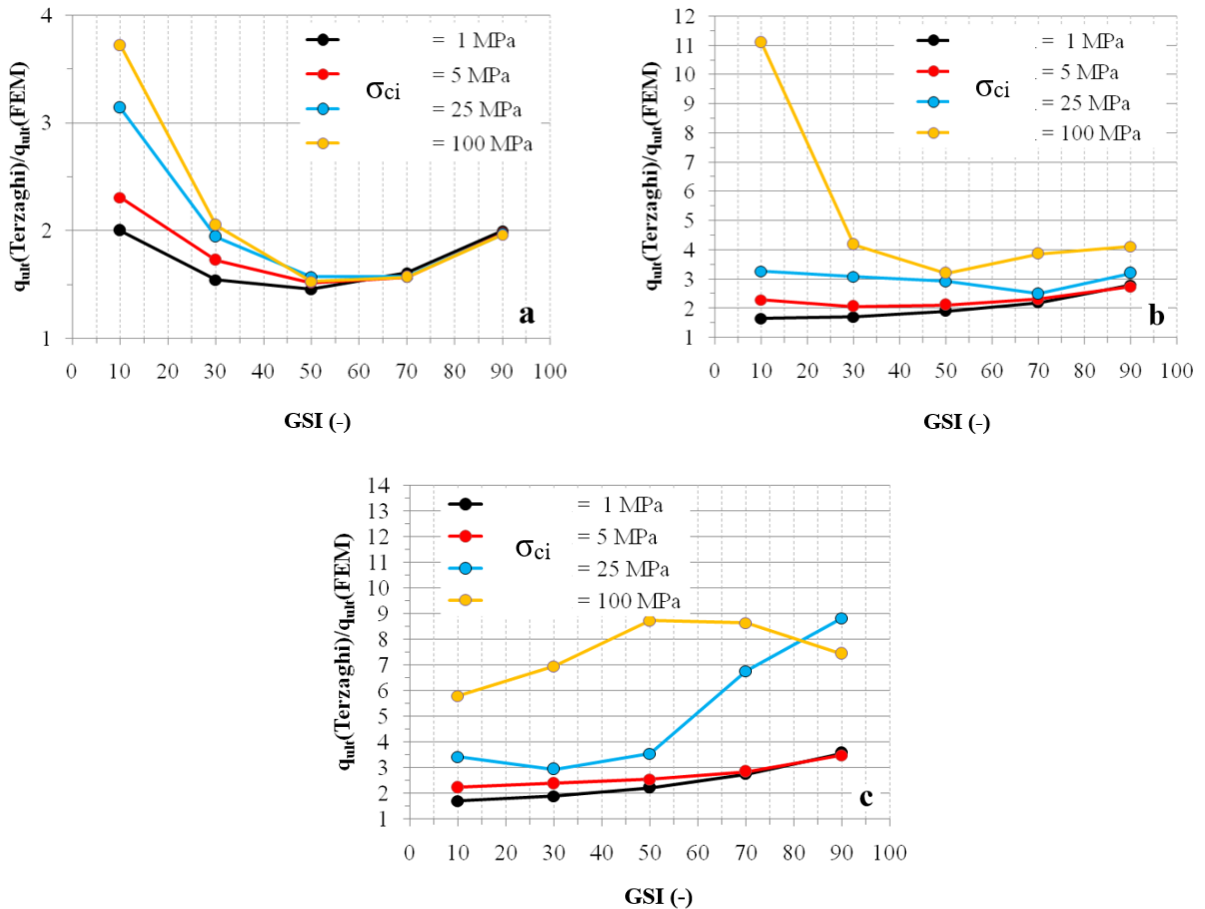

Fig. 4. Comparison of the ultimate bearing capacities obtained from the FEM and Terzaghi`s method: a) m_i = 2.5, b) m_i =10, c) m_i =20.

In cases in which the unconfined compressive strength of the intact rock σ_{ci} is relatively low ($\sigma_{ci} \leqslant$ 5 MPa with m_i = 2.5-20 and $\sigma_{ci} \leqslant$ 25 MPa with m_i < 20), the ratio of the ultimate bearing capacity calculated according to the Terzaghi`s approach $q_{ult\ (Terzaghi)}$ to those in the FEM $q_{ult\ (FEM)}$ varies between 1.5 and 4. In cases in which the value of σ_{ci} is higher (σ_{ci} = 25 MPa with m_i = 20 and GSI > 50 as well as σ_{ci} > 25 MPa with m_i > 2.5), the ratio of $q_{ult\ (Terzaghi)}$ / $q_{ult\ (FEM)}$ varies between 3 and 11 (Fig. 4). This increase can be explained by the developing of more different failure surfaces shown in Figures 3b and 3c than the general shear failure suggested by Terzaghi in Fig. 2a.

4. Conclusions

In the present study, the ultimate bearing capacity of a strip footing constructed on rock masses with different material properties (σ_{ci} = 1 to 100 MPa, m_i = 2.5 to 20 and GSI = 10 to 90) are estimated using the finite element

method (FEM) with Hoek & Brown failure criterion. The results of the FE-analyses are compared to those determined according to the limit equilibrium method (LEM) suggested by Terzaghi [1] and Miranda et al. [11]. The analyses give the following results:

- The Terzaghi`s approach gives the highest values of ultimate bearing capacities while the lowest values are obtained from the approach of Miranda;
- In most cases, especially in cases in which the unconfined compressive strength of the intact rock is relatively low ($\sigma_{ci} \leqslant 5$ MPa with $m_i = 2.5$-20, $\sigma_{ci} \leqslant 25$ MPa with $m_i < 20$), the FEM and the Terzaghi`s method give the similar failure surfaces. In these cases, the ratio of the ultimate bearing capacities obtained from the Terzaghi´s method q_{ult} (Terzaghi) to those in the finite element method q_{ult} (FEM) varies between 1.5 and 4.
- In cases in which the value of σ_{ci} is relatively high ($\sigma_{ci} = 25$ MPa with $m_i = 20$ and GSI > 50 as well as $\sigma_{ci} >$ 25 MPa with $m_i > 2.5$), the ratio of $q_{ult(Terzaghi)} / q_{ult(FEM)}$ can rise up to 11;
- The relatively high ratios of $q_{ult(Terzaghi)} / q_{ult(FEM)}$ appear especially for rock masses with high unconfined compressive strengths ($\sigma_{ci} \geq 25$ MPa), which can be explained that the rocks with relatively low compressive strengths behave like soils.

Finally, it should be mentioned that the loads corresponding to the ultimate bearing capacity of footings can lead to high deformations, which may be not allowed. The most important advantage of the FEM compared to the LEM is that it enables the estimation of deformations of rock masses under foundation loads. However, the correct estimation of the dilatant behaviour of rock masses has an essential role in accuracy of the FE-results. Thus, sensitivity analyses are necessary with respect to the value of maximum dilatancy angle on rock surface and its variation with depth.

Acknowledgements

References

[1] K. Terzaghi, *Theoretical soil mechanics*. New York, USA: John Wiley & Sons, 1943.
[2] D.C. Wyllie, *Foundations on Rock*. London: E & FN Spon and USA and Canada: Routledge, 1999.
[3] A. Serrano, C. Ollala, and J. Gonzalez, "Ultimate bearing capacity of rock masses based on the modifed Hoek
Brown criterion," *International Journal of Rock Mechanics & Mining Sciences*, vol. 37, no. 6, pp. 1013–1018, September 2000, doi:10.1016/S1365-1609(00)00028-9.
[4] X. Yang and J.H. Yin, "Upper bound solution for ultimate bearing capacity with a modified Hoe-Brown failure
Criterion," *International Journal of Rock Mechanics & Mining Sciences*, vol. 42, no. 4, pp. 550–560, June 2005, doi: 10.1016/j.ijrmms.2005.03.002.
[5] R.S. Merifeld, A.V. Lyamin, and S.W. Sloan, "Limit analysis solutions for the bearing capacity of rock masses
using the generalised Hoek-Brown criterion," *International Journal of Rock Mechanics & Mining Sciences,* vol. 43, no. 6, pp. 920–937, September 2006, doi: 10.1016/j.ijrmms.2006.02.001.
[6] Z. Saada, S. Maghous, and D. Garnier, "Bearing capacity of shallow foundations on rocks obeying a modified
Hoek–Brown failure criterion," *Computers and Geotechnics*, vol. 35, no. 2, pp. 144-154, March 2008, doi: 10.1016/j.compgeo.2007.06.003.
[7] Eurocode 7, *Geotechnical Design–Part 1: General Rules*. CEN, Brussels: 2004.
[8] J.E. Bowles, *Foundation Analysis and Design*. Singapore: McGraw Hill, 1996.
[9] E. Hook, C. Carranza-Torres, and B. Corkun, "Hoek-Brown failure criterion-2002 edition," in *Proc. of the
North American rock mechanics society meeting*, 2002, October 267-273, 2002. [Online]. Available: https://www.rocscience.com/assets/resources/learning/hoek/Hoek-Brown-Failure-Criterion-2002.pdf.
[10] E. Hoek and E.T. Brown, "The Hoek-Brown failure criterion and GSI-2018 edition," *Journal of Rock Mechanics
and Geotechnical Engineering,* vol. 11, no. 3, pp. 445-463, June 2019, doi: 10.1016/j.jrmge.2018.08.001.
[11] T. Miranda, F. Martins, and N. Araujo, "Design of spread foundations on rock masses according to Eurocode 7,"
in 12th ISRM Congress, 2011, pp. 1959-1962, doi: 10.1201/b11646-373.
[12] A.H. Javid, A. Fahimifar, and M. Imani, "Numerical investigation on the bearing capacity of two interfering

strip footings resting on a rock mass," *Computers and Geotechnics*, vol. 69, pp. 514-528, September 2015, doi: 10.1016/j.compgeo.2015.06.005.

[13] M. Mansouri, M. Imani, and A. Fahimifar, "Ultimate bearing capacity of rock masses under square and rectangular footings," *Computers and Geotechnics,* 111, pp. 1-9, July 2019, doi: 10.1016/j.compgeo.2019.03.002.

[14] S. Shamloo and M. Imani, "Upper bound solution for the bearing capacity of rock masses considering the embedment depth," *Ocean Engineering*, vol. 218, no. 6, December 2020, doi: 10.1016/j.oceaneng.2020.108169.

[15] G. Wu, M. Zhao, R. Zhang, and G. Liang, "Ultimate bearing capacity of eccentrically loaded strip footings above voids in rock masses," *Computers and Geotechnics,* vol. 218, December 2020, doi: 10.1016/j.compgeo.2020.103819.

[16] H. Chen, H. Zhu, and L. Zhang, "An analytical approach to the ultimate bearing capacity of smooth and rough strip foundations on rock mass considering three-dimensional (3D) strength," *Computers and Geotechnics*, vol. 149, no. 3, September 2022, doi: 10.1016/j.compgeo.2022.104865.

[17] M. Ranjbarnia, F. Zarei, and M. Goudarzy, "Probabilistic Analysis of Bearing Capacity of Square and Strip Foundations on Rock Mass by the Response Surface Methodology," *Rock Mechanics and Rock Engineering*, 56, pp. 343–362, vol. 56, October 2022, doi: 10.1007/s00603-022-03090-5.

[18] S. Das and D. Chakraborty, "Effect of eccentric and inclined loading on the bearing capacity of strip footing placed on rock mass," *Journal of Mountain Science*, vol. 21, pp. 292–312, January 2024, doi: 10.1007/s11629-023-8312-2.

[19] H. Chen, H. Zhu, and L. Zhang, "Semi-analytical solution for ultimate bearing capacity of smooth and rough circular foundations on rock considering three-dimensional strength," *International Journal for Numerical and Analytical Methods in Geomechanics*, February 2024, doi: 10.1002/nag.3699.

[20] Plaxis 2D, Delft: Plaxisbv, 2019.

[21] M. Singh, M.N. Viladkar, P.S. Shekhawat, K. Tripathi, and M. Amin, "Bearing capacity of strip footings on jointed rock mass," Arabian Journal of Geosciences, vol. 15, September 2022, doi: 10.1007/s12517-022-10841-9.

[22] B.M. Das, *Principles of Foundation Engineering*. Boston, USA: Cengage Learning, 2014.

[23] RocData, version 5.0, Toronto: Rocscience Inc., 2019.